Upregulated enhancer of rudimentary homolog promotes epithelial-mesenchymal transition and cancer cell migration in lung adenocarcinoma

YING-MING TSAI[1-3], KUAN-LI WU[1-3], YUNG-CHI HUANG[1,3], YU-YUAN WU[4], CHAO-YUAN CHANG[1,5], YUNG-YUN CHANG[2,6], HUNG-HSING CHIANG[7], LIAN-XIU LIU[1] and JEN-YU HUNG[1-3,8]

[1]Graduate Institute of Medicine, College of Medicine; [2]Division of Pulmonary and Critical Care Medicine, Kaohsiung Medical University Hospital; [3]Drug Development and Value Creation Research Center; [4]School of Medicine, College of Medicine, Kaohsiung Medical University; [5]Department of Anatomy; [6]Division of General Medicine, Kaohsiung Medical University Hospital; [7]Division of Thoracic Surgery, Department of Surgery, Kaohsiung Medical University Hospital, Kaohsiung Medical University; [8]Department of Internal Medicine, Kaohsiung Municipal Ta-Tung Hospital, Kaohsiung 807, Taiwan, R.O.C.

Received October 14, 2022; Accepted July 21, 2023

DOI: 10.3892/mmr.2023.13132

Abstract. Lung adenocarcinoma (LUAD) is one of the deadliest cancers regarding both mortality rate and number of deaths and warrants greater effort in the development of potential therapeutic targets. The enhancer of rudimentary homolog (*ERH*) has been implicated in the promotion and progression of certain types of cancer. In the present study, *ERH* was assessed for its expression pattern and survival association with LUAD in public transcriptomic and proteomic databases. Bioinformatic methods and data from websites, including University of Alabama at Birmingham CANcer data analysis Portal and The Cancer Genome Atlas, were utilized to demonstrate the functional behaviors and corresponding pathways of ERH in LUAD. Human A549 and CL1-0 cell lines were used to validate the findings via functional assays. It was demonstrated that the expression of ERH, at both the transcriptomic and proteomic levels, was higher in LUAD compared with in adjacent non-tumor lung tissue and was associated with worse survival prognosis. Moreover, high *ERH* expression was correlated with more aggressive functional states, such as cell cycle and invasion in LUAD, and the positive *ERH*-correlated gene set was associated with worse survival and an immunosuppressive tumor microenvironment. Small nuclear ribonucleoprotein polypeptide G was identified as a molecule that potentially interacted with *ERH*. Lastly, it was demonstrated that ERH promoted epithelial-mesenchymal transition and cell migration *in vitro*, but not proliferation. In conclusion, higher expression of ERH in LUAD may facilitate cancer progression and confer worse outcomes. Further deep investigation into the role of ERH in LUAD is needed.

Correspondence to: Professor Jen-Yu Hung, Graduate Institute of Medicine, College of Medicine, Kaohsiung Medical University Hospital, 100 Shih-Chuan 1st Road, Kaohsiung 807, Taiwan, R.O.C.
E-mail: jyhung@kmu.edu.tw

Key words: lung adenocarcinoma, epithelial-mesenchymal transition, migration, ERH

Introduction

Lung cancer is the leading cause of cancer deaths worldwide due to its high mortality rate (1), with lung adenocarcinoma (LUAD) as the most frequently occurring subtype, accounting for 38.5% of lung cancer cases (2). Efforts have been made to improve the survival outcome for patients with lung cancer, with effective measures including the implementation of lung cancer screening by low-dose computed tomography (3), the detection of potential druggable genetic alterations by modern sequencing methods, and the invention and application of new targeted therapies and immune checkpoint inhibitors (4,5). Although these measures have modified and improved the clinical outcomes, such as overall survival, for patients with lung cancer, ~70% of patients with lung cancer are still diagnosed at an advanced stage of disease (6) and with the prognosis falling below expectations, despite these modern strategies (7). To improve the clinical outcomes, clinicians should further evaluate experimental treatments and outcomes to develop more effective therapeutic options for LUAD.

The enhancer of the rudimentary homolog (*ERH*) is a protein-coding gene analog that is highly conserved across species. For example, human *ERH* is ~80% identical to its protein analog in *Drosophila melanogaster*, DROER (8), located at chromosome 14 and with a size of ~18,000 base pairs (9). The translated protein is comprised of 104 amino acids, and it is mostly localized to the nucleus (10). It is involved in numerous fundamental biological processes, such as the pyrimidine metabolic pathway, transcription control, cell cycle progression, DNA damage response and repair, and mRNA splicing (11), whilst additionally interacting with RNA Pol II-associated factors that are involved in microRNA

processing (12). The family of small nuclear ribonucleoprotein polypeptides (SNRPs) has a crucial role in tumorigenesis and its progression (13). Notably, ERH has been shown to interact with the spliceosome protein, SNRPD3, and is required for the mRNA splicing of centrosome-associated protein E (CENP-E) (14).

ERH has been studied for its role in malignancy since 2007, and to date, its upregulation has been reported in numerous cancers, such as breast, ovarian and bladder cancer (15). *ERH* upregulation is associated with poor clinical outcomes in ovarian cancer (16) and colorectal cancer (9); however, a conflicting report illustrated a favorable outcome in patients with gastric carcinoma with upregulated *ERH* (17). Cell behaviors influenced by *ERH* in cancer have not been widely studied (18), although existing evidence has revealed the association between *ERH* and cell proliferation, inhibition of apoptosis, migration, invasion and epithelial-mesenchymal transition (EMT) in different cancer types (19). The roles of *ERH* in LUAD remain unknown or only partially explored (15), with further elucidation of the expression pattern, prognostic implications and its functional roles in pathogenesis required.

Advanced lung cancer, compared with early-stage lung cancer, carries the worst clinical outcomes despite efforts invested (20) and further efforts are required to improve clinical outcomes, such as survival time. The present study suggests that high-level expression of *ERH* confers poor survival time in patients with LUAD with the most plausible mechanisms dependent on the recruitment of immunosuppressive cells such as myeloid-derived suppressor cells (MDSCs) and regulatory T lymphocytes (Tregs), and enhancement of invasive cellular functions such as migration and EMT. The results of the present study elucidate the role of *ERH* in LUAD and modifying its expression might be of potential benefit as a target in lung cancer treatment.

Materials and methods

Patient sample collection. Eighteen participants diagnosed with LUAD were recruited from January 2018 to December 2022 at the Division of Thoracic Surgery and Division of Pulmonary and Critical Care Medicine, Kaohsiung Medical University Hospital [approval nos. KMUH-IRB-20180023, KMU-IRB-20200038, KMU-IRB-E(II)-20220175; Kaohsiung, Taiwan R.O.C.]. All patients provided written informed consent to participate. Eight out of eighteen paired adjacent non-tumor lung and tumor tissues (Case nos. 1-8, Table I) obtained underwent deep RNA sequencing (RNA-Seq) at a biotechnology company (Welgene, Inc.) using the Solexa platform (Illumina, Inc.). RNA and small RNA library construction was performed using a sample preparation kit (Illumina, Inc.), following the protocol of the TruSeq RNA or Small RNA Sample Preparation Guide. Data were submitted to the National Center for Biotechnology Information Gene Expression Omnibus (GEO) under accession number GSE236816.

Immunohistochemical staining (IHC). Ten pairs of adjacent non-tumor lung tissues and lung cancer tissues (Case nos. 9-18, Table I) were utilized for IHC. The designated tissue samples were fixed with 10% formalin at room temperature for 1 h and the tissue block was embedded in paraffin. The formalin-fixed paraffin-embedded tissue block was then split into sections (8 μm). Xylene was used to dewax the sections and a descending ethanol gradient was used for rehydration. Antigen retrieval was heat-mediated using a pressure cooker for 90 sec. Endogenous peroxidase activity was inactivated by incubation with 3% hydrogen peroxide for 10 min at room temperature, and non-specific antibody binding was prevented by incubation with 3% bovine serum albumin (MilliporeSigma) for 20 min at room temperature. The sections were incubated with primary antibodies against ERH (1:200; cat. no. NBP1-84976; Novus Biologicals, LLC) and small nuclear ribonucleoprotein polypeptide G (SNRPG; 1:500; cat. no. PA5-64155; Invitrogen; Thermo Fisher Scientific, Inc.) to assess ERH and SNRPG protein expression at 4˚C overnight followed by incubation with horseradish peroxidase conjugated anti-rabbit secondary antibodies (1:1,000; cat. no. ab6721, Abcam) for 20 min at room temperature, followed by washing with PBS and 3,3' diaminobenzidine staining for 2 min at room temperature. The sections were counterstained with hematoxylin for 1 min at room temperature. The results of IHC were imaged using an ICC50 HD light microscope (Leica Microsystems, Inc.) at x100 magnification.

Data validation using in-house samples by reverse transcription-quantitative PCR (RT-qPCR) and IHC. To validate the findings from the public database, the present study collected 8 human LUAD tumor tissues and adjacent non-tumor tissues. Total RNA was extracted from tissues or cell lines using TRIzol® reagent (Invitrogen; Thermo Fisher Scientific, Inc.), and 50 ng mRNA was reverse transcribed into cDNA using an oligo (dT) primer and reverse transcriptase (PrimeScript RT Reagent Kit; Takara Bio, Inc.) according to the manufacturer's protocols. RT-qPCR was performed on the human samples to quantify the *ERH* mRNA expression levels. The primers used in the experiment were as follows: ERH forward (F), ERH_ F1, 5'-CCTACCAAGAGGCCAGAAGG-3' and reverse (R), ERH_ R1, 5'-TAAACCAGGCAGCTGAGGTC-3'; GAPDH F, 5'-TTCACCACCATGGAGAAGGC-3' and R, 5'-GGCATGGACTGTGGTCATGA-3'). qPCR was performed at 95˚C for 20 sec, followed by 40 cycles at 95˚C for 3 sec and 60˚C for 30 sec. The expression levels of specific genes were determined using a StepOne-Plus PCR instrument (Applied Biosystems; Thermo Fisher Scientific, Inc.) and SYBR-Green (Thermo Fisher Scientific, Inc.). The relative expression levels of the specific mRNAs were normalized to those of GAPDH. The relative standard method ($2^{-\Delta\Delta Cq}$) was used to calculate relative RNA expression (21).

Data collection from public databases. The gene expression profile of LUAD was obtained from The Cancer Genome Atlas (TCGA) via the University of Santa Cruz Xena database (https://xenabrowser.net/datapages/?host=https%3A%2F%2Fpancanatlas.xenahubs.net&removeHub=https%3A%2F%2Fxena.treehouse.gi.ucsc.edu%3A443; accessed on June 15, 2022). For the protein expression pattern in LUAD, data were extracted from The Human Protein Atlas website (https://www.proteinatlas.org/ENSG00000100632-ERH/pathology/lung+cancer#img; accessed on June 22, 2022). In the TCGA cohort, there were 2 tissues from healthy patients, 57 pairs of adjacent non-tumor and tumor tissues, and 454 tumor tissues (total normal tissue, n=59; total tumor tissues, n=511). Further analysis of the gene and protein expression pattern across tissue types, cancer stages

Table I. Patients' clinicopathological data.

Case number	Age	Sex	Pathologic findings	Stage (Tumor, Node and Metastasis)
1	46	F	Adenocarcinoma	1A (T1N0M0)
2	50	F	Adenocarcinoma	1A (T1aN0M0)
3	58	F	Adenocarcinoma	1A (T1aN0M0)
4	63	M	Adenocarcinoma	1B (T2aN0M0)
5	64	F	Adenocarcinoma	1A (T1aN0M0)
6	48	M	Adenocarcinoma	1A (T1aN0M0)
7	82	M	Adenocarcinoma	4 (T1bN2M1b)
8	62	F	Adenocarcinoma	4 (T1bN0M1b)
9	75	M	Adenocarcinoma	2B (T2bN1M0)
10	65	F	Adenocarcinoma	3A (T2aN2M0)
11	66	M	Adenocarcinoma	1A (T1aN0M0)
12	70	F	Adenocarcinoma	1B (T2aN0M0)
13	75	F	Adenocarcinoma	2B (T2bN1M0)
14	50	M	Adenocarcinoma	1B (T1bN0M0)
15	63	F	Adenocarcinoma	1A (T1aN0M0)
16	57	F	Adenocarcinoma	2B (T1N1M0)
17	76	M	Adenocarcinoma	2B (T2bN1M0)
18	65	M	Adenocarcinoma	1A (T1aN0M0)

and the extent of lymph node metastasis were extracted from the public platform, the University of Alabama at Birmingham CANcer data analysis Portal [the Clinical Proteomic Tumor Analysis Consortium (CPTAC) and the International Cancer Proteogenome Consortium datasets, UALCAN; http://ualcan.path.uab.edu]. The gene sets which correlated, either positively or negatively, with *ERH* were also identified using the UALCAN platform using the cutoff correlation co-efficiency r>0.3 or r <-0.3, respectively. To validate the gene expression results from TCGA, the Asian cohort GSE31210 dataset (control=20, with 15 from adjacent non-tumor tissues and 5 from normal tissues from healthy individuals; tumor=226) from the GEO (https://www.ncbi.nlm.nih.gov/geo/query/acc.cgi?acc=GSE31210) was used with MAS5 normalization (22). STRING is a database of known and predicted protein-protein interactions for numerous genes, including for *ERH* (https://string-db.org/; version 11.5, accessed on June 15, 2022).

Cell cultures. The Human A549 LUAD cell line (American Type Culture Collection; CCL185) was cultured in F-12K Medium (Thermo Fisher Scientific, Inc.) supplemented with 10% fetal bovine serum (FBS; Gibco; Thermo Fisher Scientific, Inc.), 0.1 mg/ml streptomycin and 100 U/ml penicillin (Thermo Fisher Scientific, Inc.). Human CL1-0 LUAD cell line was donated by Professor Pan-Chyr Yang (National Taiwan University, College of Medicine, Taiwan). The CL1-0 cell line was cultured in RPMI 1640 medium supplemented with 10% FBS, 2 mM glutamine and 1% penicillin-streptomycin (Capsugel; Lonza Group, Ltd.). Both cell lines were confirmed negative for mycoplasma contamination using mycoplasma test kits (Mycoalert Mycoplasma Detection Kit; Capsugel; Lonza Group, Ltd.) every 3 months.

Survival analysis of selected genes using the Kaplan-Meier plotter (KM plotter). The effect on survival of the genes of interest was evaluated using the KM plotter (http://kmplot.com/analysis/; accessed on June 19, 2022) using data sourced from the TCGA and GEO databases. In the survival analysis of LUAD in the KM plotter, data from gene chip microarray or RNA-Seq were used. Subjects were divided into two groups based on their high or low RNA expression levels, with the best cutoff value automatically computed. The hazard ratios for survival, including overall survival, time to first progression and post-progression survival, were calculated using the Cox proportional-hazards model during a pre-defined 60-month period. In addition, cross-analysis was utilized to compare the survival rates between patient cohorts with high and low expression of a specific gene (bisection) (http://kmplot.com/analysis/) (23). P<0.05 was considered to indicate a statistically significant difference.

Functional analysis. The biological functions of *ERH* were evaluated using CancerSEA (http://biocc.hrbmu.edu.cn/CancerSEA/home.jsp; accessed on June 8, 2023). Gene set enrichment analysis (GSEA) is a computational tool that computes correlations between biological functions or pathological states with a pre-defined gene set. In the present study, the subjects in the TCGA LUAD cohort were divided into *ERH* high- and low-expression groups that were defined as the 1st and 4th quartiles (highest 25% and lowest 25%) to enhance the significance. GSEA was then used to analyze the enrichment of biological functions in *ERH* high- and low-expression groups. A false discovery rate of <0.05 and P<0.05 were set as the cutoff criteria. The gene set 'c2.cp.kegg.v6.2.symbols.gmt' was used as the reference.

Gene set analysis in Gene Set Variation Analysis (GSVA) and Metascape. The gene sets either positively or negatively correlated with *ERH* were extracted using UALCAN. The criteria set

for the analysis were Pearson correlation coefficient >0.3/<-0.3 and P<0.05, which were calculated using UALCAN. The GSVA score of the gene sets with regards to gene expression, survival rate and immune infiltration was calculated using Gene Set Cancer Analysis (GSCA) (24) (http://bioinfo.life.hust.edu.cn/GSCA/#/; accessed on July 19, 2022). Metascape (https://metascape.org/gp/index.html#/main/step1; version 3.5, accessed on July 23, 2022) was also used to provide a comprehensive gene list annotation and analysis for the *ERH*-positively correlated gene set. The correlated pathways enriched with the target gene list were presented as a heatmap and a clustergram (25).

Analysis of the ERH-associated immune microenvironment. Tumor Immune Estimation Resource 2.0 (TIMER2.0; http://timer.cistrome.org/; accessed on July 15, 2022) was used for the analysis of *ERH*-associated infiltrating immune cells (26). The 'gene module' was used to select and visualize *ERH* protein expression with its correlated immune cell infiltration level in LUAD. GSCA was also utilized for immune cell abundance analysis of the *ERH*-positively or negatively correlated gene set (22). Using the 'Immune cell abundance' module, the correlation between immune infiltration and the calculated GSVA score was calculated.

ERH knockdown by siRNA transfection. A549 and CL1-0 cells were transfected with *ERH*-siRNA or control-siRNA (10 nM) using ON-TARGET plus SMARTpool siRNA and Dharmafect reagents No1 (GE Healthcare Dharmacon, Inc.) at 37˚C for 48 h. The knockdown efficacy of *ERH* siRNA was determined by RT-qPCR at 48 h post-transfection according to aforementioned methods, respectively. The sequences were as follows: control siRNA: UGGUUUACAUGUCGACUAA, UGGUUUACAUGUUGUGUGA, UGGUUUACAUGUUUUCUGA and UGGUUUACAUGUUUUCCUA and *ERH*-siRNA: AGACAUACCAGCCUUAUAA, GGGAAAUAAUUGUGUUGGA, AAGAGAAGAUCUACGUGCU and UAGCCAAGAUUGACUGUAU, respectively. The subsequent experiments were performed 48 h post-transfection.

Cell proliferation assay. The cell proliferation of control siRNA or *ERH* siRNA transfected A549 cells and CL1-0 cells were assessed using the WST-1 assay (MilliporeSigma) for a 72 h incubation, according to the manufacturer's protocol.

Wound healing assay. A total of $2x10^5$ *ERH* siRNA or control-siRNA transfected A549 and CL1-0 cells were seeded and allowed to grow to ~90% confluence in 24-well plates cultured in media which contained 1% FBS (27). The following day, a uniform scratch was made down the center of the well using a micropipette tip, followed by washing once with phosphate-buffered saline (PBS). Imaging of wound healing at 0 and 24 h was performed using an Olympus inverted light microscope.

Cell migration assay. A cell migration assay was performed using a Transwell system, as previously described (28). Briefly, $3x10^4$ *ERH* siRNA and control siRNA transfected A549 and CL1-0 cells were seeded into the top inserts with serum-free medium and incubated for 10 min and complete medium containing 10% FBS was placed in the bottom well and cultured at 37˚C in an incubator. After 24 h, the migratory cells on the bottom of inserts then were fixed in 4% paraformaldehyde for 20 min at room temperature and stained with 0.1% crystal violet overnight at room temperature. The migratory cells were counted in 10 random microscope fields for each sample using a light microscope (Nikon Corporation).

Western blotting. The total protein of *ERH*-knockdown and control A549 and CL1-0 cells was extracted using RIPA buffer (cat. no. 20-188; MilliporeSigma), supplemented with a protease inhibitor mixture (S8830-20TAB, MilliporeSigma). An equal volume of total protein, 25 μg, was denatured by heating and then separated by electrophoresis using 12% sodium dodecyl-sulfate polyacrylamide gels. Proteins in the gel were transferred onto polyvinylidene difluoride membranes (MilliporeSigma) by electroblotting, which was probed with primary antibodies overnight after blocking in 5% non-fat dry milk/0.1% TBST at room temperature (25˚C). Primary antibodies against N-cadherin (1:1,000; cat. no. 610921), E-cadherin (1:1,000; cat. no. 610182), and Vimentin (1:1,000; cat. no. 550513) were purchased from Becton, Dickinson and Company. Anti-*ERH* antibodies (1:1,000; cat. no. NBP1-84976) were purchased from Novus Biologicals, LLC and anti-GAPDH (1:5,000; cat. no. MAB374) antibodies were from MilliporeSigma. After incubation with HRP-conjugated secondary antibodies (1:5,000; anti-mouse, cat. no. 7076; anti-rabbit, cat. no. 7074; Cell Signaling Technology, Inc.). The signal of the specific protein was detected using a chemiluminescence kit (MilliporeSigma). The western blot was semi-quantified using ImageJ (version 1.53; National Institutes of Health) and each experiment was repeated independently at least three times.

Statistical analysis. The raw data extracted from GSE31210 and the results of the cell functional assays were re-plotted using GraphPad Prism 5 software (GraphPad Software; Dotmatics). One-way ANOVA was used for analysis when comparing more than two groups with Tukey's post hoc test. Unpaired Student's t-test was used to compare mean values between different subjects and cell groups. P<0.05 was considered to indicate a statistically significant difference.

Results

Higher expression of ERH in LUAD confers a poor prognosis. Using the public transcriptomic database TCGA, the mRNA-Seq profile of LUAD was obtained and the levels of *ERH* mRNA expression were demonstrated to be significantly higher in tumor tissues (n=511) than in the adjacent non-tumor tissues (n=59) (Fig. 1A). Significantly elevated *ERH* expression was demonstrated across different tumor stages and at different extents of lymph node involvement, although the increase did not demonstrate stage- or lymph node stage-dependence (Fig. 1B and C). To validate these findings in the in-house cohort, RT-qPCR for *ERH* was performed. Higher *ERH* expression in tumors was demonstrated in 6 out of 8 samples, ranging from a $\log_2$ fold change of 1.26 to 1.71 compared with the adjacent non-tumor baseline; by contrast, *ERH* expression was lower in 2 of the 8 samples (Fig. 1D).

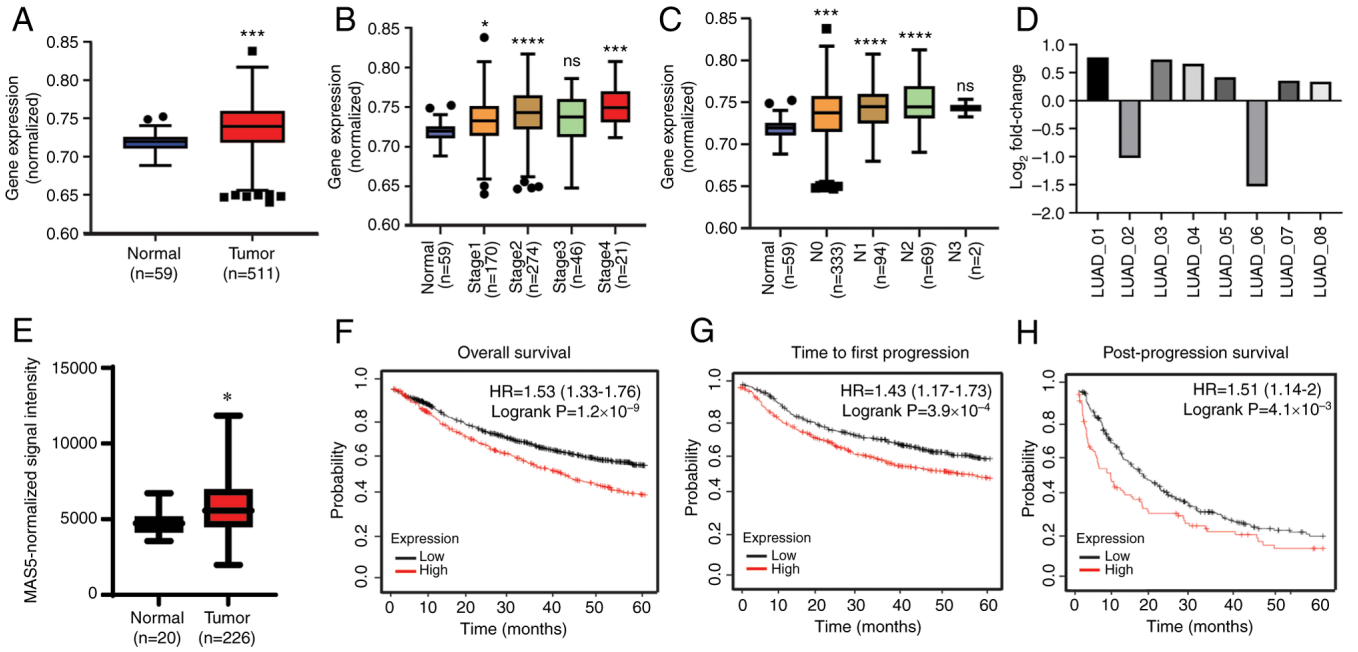

Figure 1. High expression of ERH in LUAD confers poor prognosis. The levels of *ERH* mRNA expression in non-tumor tissues vs. tumor tissues using the (A) TCGA LUAD transcriptomic dataset, (B) tumor stages, and (C) extents of lymph node involvement. N1, ipsilateral hilum; N2, ipsilateral mediastinal or subcarinal lymphadenopathy; N3, contralateral mediastinal or contralateral hilar lymphadenopathy or scalene or supraclavicular node. (D) *ERH* expression in eight pairs of adjacent non-tumor vs. tumor in-house LUAD samples and (E) non-tumor tissues vs. tumor tissues in a public transcriptomic profile of LUAD, GSE31210, after MAS5 normalization. Survival analysis based on *ERH* expression in LUAD in terms of (F) overall survival, (G) time to first progression and (H) post-progression survival. *P<0.05; ***P<0.005; ****P<0.001 vs. normal. ERH, enhancer of rudimentary homolog; LUAD, lung adenocarcinoma; TCGA, The Cancer Genome Atlas; HR, hazard ratio.

The results were also validated in another public transcriptomic dataset, GSE31210, to assess the association between *ERH* expression and ethnicity. This dataset exclusively includes an Asian population and similarly, the expression of *ERH* was significantly increased in the tumor tissues (n=226) compared with the mixed healthy and adjacent normal tissues [paired adjacent non-tumor tissues (n=15) and normal tissues from healthy individuals (n=5)] (P<0.05; Fig. 1E). Moreover, the level of *ERH* expression in LUAD was significantly linked with worse outcomes (Fig. 1F-H). The prognostic profiles regarding overall survival, time to first progression and time of post-progression survival were obtained from the KM plotter and as illustrated, for the higher levels of *ERH* expressed in tumors, a significantly lower probability of each survival parameter was notably demonstrated in the pre-defined 60-month period. To summarize, higher levels of *ERH* were expressed in tumor tissues compared with those in normal tissues across different ethnicities and higher expression levels of *ERH* were significantly associated with reduced survival times. This indicated that *ERH* may serve a critical role in LUAD.

ERH protein expression is upregulated in LUAD. The ERH protein expression pattern in LUAD was further evaluated. The proteomic data obtained from the CPTAC demonstrated a significantly enhanced expression pattern of ERH protein in tumor tissues compared with adjacent non-tumor tissues (median Z-score, 0.027 vs. -0.613; Fig. 2A). IHC staining images in the Human Protein Atlas demonstrated that there was a higher intensity of ERH expression in tumors compared with in normal tissues (healthy control) (Fig. 2B). These results indicated that *ERH* might be critical in LUAD at the protein level observed in the public cohorts and the in-house cohort.

ERH expression correlates with aggressive functional states in LUAD. The CancerSEA website was utilized to elucidate the corresponding biological function of *ERH*. It was demonstrated that in LUAD, *ERH* expression was significantly positively correlated with a broad range of functional behaviors towards cancer progression, such as angiogenesis, apoptosis, cell cycle, differentiation, DNA damage, DNA repair, EMT, hypoxia, invasion, metastasis, proliferation, and stemness. Among these, DNA damage/repair, cell cycle and invasion were the most correlated aggressive functions with *ERH* expression after setting a cutoff correlation strength of 0.3 (Fig. 3A). Furthermore, when linked to biological processes such as cell cycle, proliferation, invasion, EMT and metastasis using the GSEA method in lung cancer, the *ERH*-correlated gene set was strongly associated with poor survival and chemo-resistance (Fig. 3B). This bioinformatics evidence demonstrated the roles of ERH in DNA damage/repair, cell cycle and invasion of LUAD progression.

SNRPG potentially interacts with ERH. Ten molecules that potentially interact with *ERH* were identified using the STRING database data on protein-protein interactions. These molecules included DDX39B, CHTOP, HNRNPH1, MATR3, SNRPD1, SNRPD2), SNRPD3, SNRPE, SNRPF, and SNRPG (Fig. 4A). Moreover, all were strongly correlated with *ERH* expression in the TCGA LUAD dataset with a correlation strength r>0.4 (Fig. 4B). Among the potentially interactive factors, the upregulation of *SNRPD1, SNRPD2, SNRPD3,*

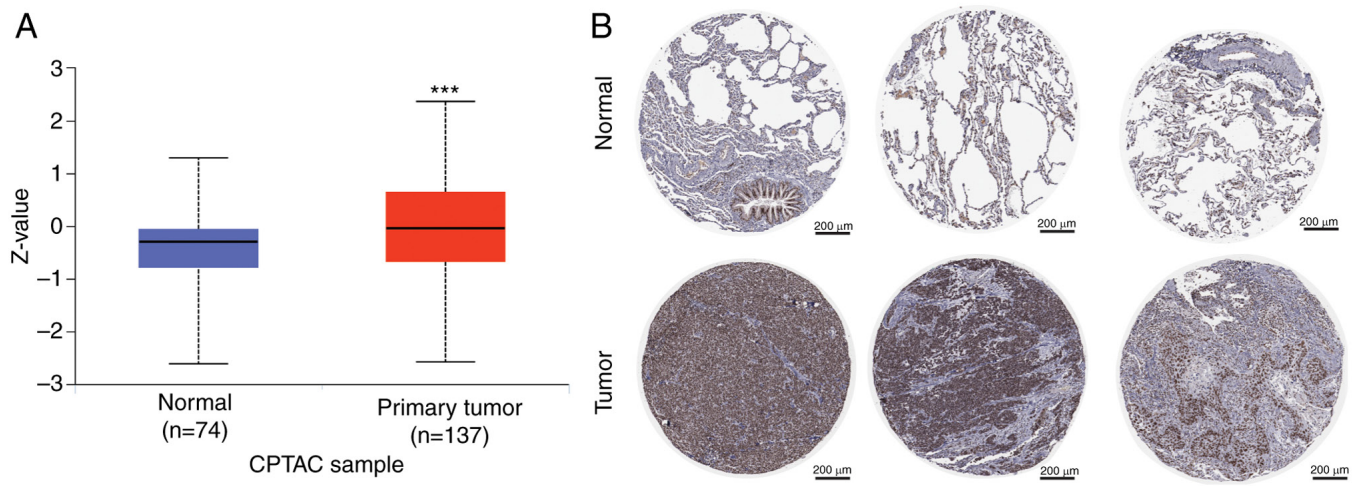

Figure 2. Expression of ERH protein in LUAD. (A) ERH protein expression of normal and tumor tissue from data obtained from the CPTAC database. (B) Immunohistochemistry staining of LUAD samples collected from the Human Protein Atlas ***P<0.005 compared with normal. ERH, enhancer of rudimentary homolog; LUAD, lung adenocarcinoma; CPTAC, Clinical Proteomic Tumor Analysis Consortium.

SNRPE, *SNRPF* and *SNRPG* were linked to significantly shorter survival times, determined by the best cutoff method, whereas upregulation of *MATR3* was associated with a significantly better prognosis (Fig. 4C). Survival-associated molecules were validated using the CPTAC database, from which the available protein expressions of SNRPD3, SNRPE and SNRPG were demonstrated to be significantly different between tumor and non-tumor samples, whereas SNRPD1 and SNRPD2 were expressed in similar amounts between tumor and non-tumor parts. However, only SNRPG protein demonstrated greater expression in primary tumor samples (Fig. 4D), which was in accordance with the presumed expression pattern of mRNA in the TCGA. In addition, 7 out of 10 of the tumor samples (with the exception of patient Nos 1, 8 and 9) in the in-house cohort were strongly stained by ERH or SNRPG antibodies compared with adjacent non-tumor samples. In these 7 patients, higher expression of ERH was accompanied by elevated SNRPG expression (Fig. 4E). SNRPG expression was associated with ERH expression and shorter survival duration.

The survival effect of ERH is altered by SNRPG mRNA expression levels. To assess the potential interacting effect of small nuclear ribonucleoproteins (SNRs) with *ERH*, the effect of *ERH* expression on the survival time of patients with LUAD based on high or low levels of various SNRs was evaluated using cross-analysis. Analysis using the KM plotter demonstrated that the overall survival time of patients with high *ERH* expression was significantly shorter than that of patients with low *ERH* expression in the high expression subgroups of *SNRPD2*, *SNRPD3*, *SNRPE* and *SNRPG* (Fig. 5B-D and F). These data indicated a potential *SNRPG*-dependent interaction that governed the survival impact of *ERH*.

Gene set positively correlated with ERH is associated with poor survival and an immunosuppressive tumor microenvironment (TME). The top 200 genes either positively or negatively correlated with *ERH* were extracted from the LUAD cohort of TCGA. The positive and negative gene sets were calculated via the GSCA website to acquire the GSVA scores. The scores provide the significance of the gene set in terms of survival (29). It was demonstrated that the GSVA scores for the *ERH* positively correlated gene set were significantly higher in LUAD tumor samples than normal tissue samples (Fig. 6A). Inversely, the GSVA scores for the *ERH* negatively correlated gene set were significantly lower in LUAD tumor samples than normal tissue samples (Fig. 6B). Markedly higher GSVA scores for the *ERH* positively correlated gene set were linked to advanced cancer stages (Fig. 6C). However, higher GSVA scores for the *ERH* negatively correlated gene set demonstrated a declining trend as the cancer stage advanced (Fig. 6D). Higher GSVA scores for the *ERH* positively-correlated gene set were associated with significantly worse patient outcomes in terms of overall survival (OS; HR=1.45), progression-free survival (PFS; HR=1.37) and disease-specific survival (DSS; HR=1.79), but not with disease-free survival (DFI; HR=1.28, Cox P=0.25) (Fig. 6E). In a reverse pattern, higher GSVA scores for the *ERH* negatively correlated gene set were linked to significantly better patient outcomes in terms of OS (HR=0.66) and DSS (HR=0.57), but not PFS (HR=0.78, Cox P=0.05) and DFI (HR=0.90, Cox P=0.62) (Fig. 6F). Analysis using the Metascape website demonstrated that the *ERH* positively correlated gene set was associated with certain biological processes, such as the 'cell cycle, DNA metabolic process, S phase and retinoblastoma gene in cancer' (Fig. 6G). Associated gene clusters were illustrated as an enriched ontology cluster network (Fig. 6H). Further immune microenvironment analysis was undertaken using the TIMER2.0 website, which demonstrated that *ERH* gene expression was significantly positively correlated with the infiltration of MDSCs in tumors with a ρ-value of 0.435 but not purity (ρ=0.097) (Fig. 6I). Using the GSCA website, the infiltrating immune cells corresponding to the GSVA scores for the *ERH* positively correlated gene set were demonstrated to include natural regulatory T cells (nTregs), effector memory T cells, T helper type 1 cells and exhausted T cells. Among those, nTregs demonstrated the highest correlation (Fig. 6J). The

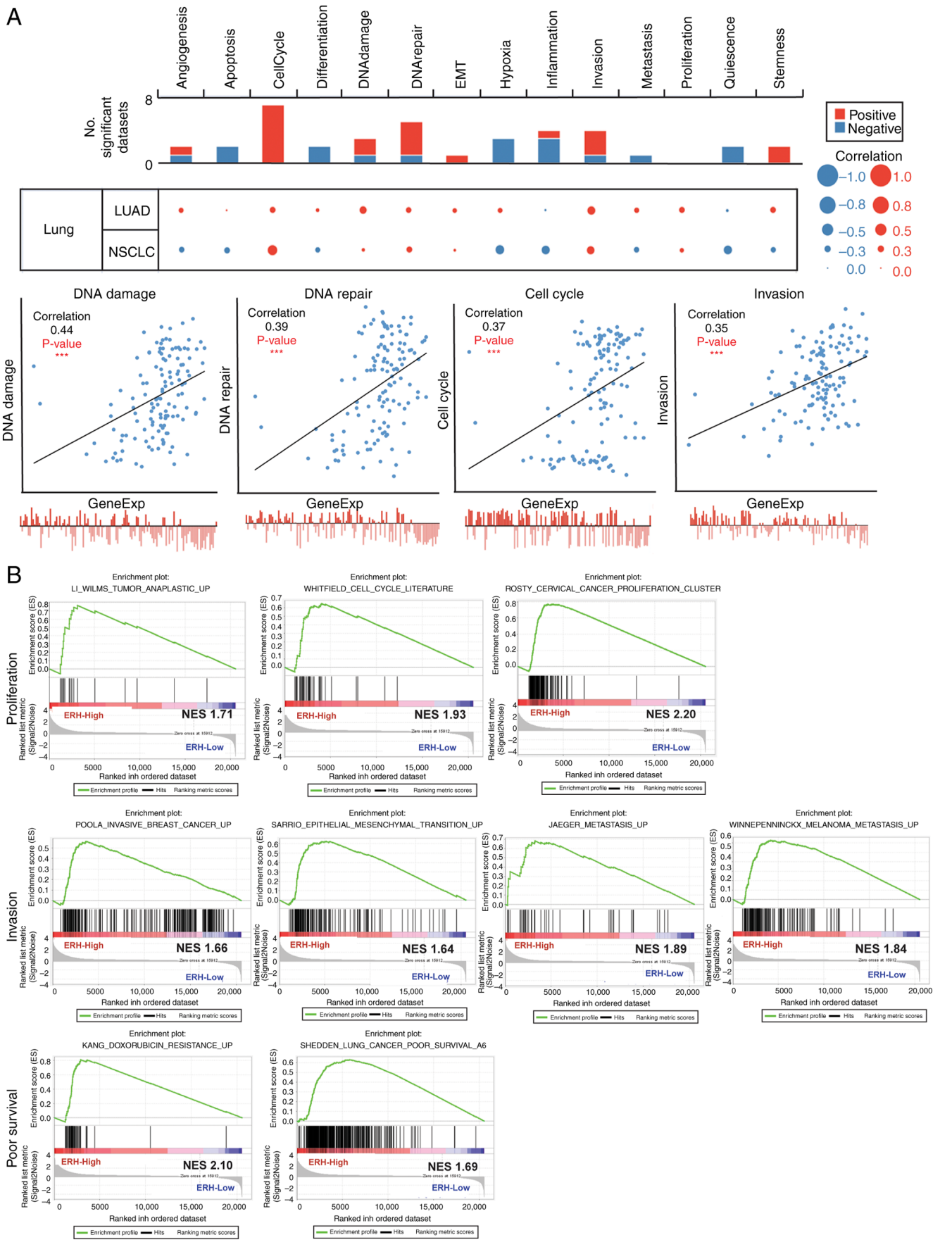

Figure 3. *ERH* expression correlates with aggressive functional states in LUAD. (A) The correlation between ERH expression and 14 functional states in LUAD, with data obtained from the CancerSEA database (upper panel). The correlation strength >0.3 (lower panel). (B) ERH-correlated gene sets and their functional behaviors toward cancer progression, such as cell cycle and proliferation (upper panel), invasiveness, epithelial-mesenchymal transition and metastasis (middle panel), and chemotherapy resistance and poor survival (lower panel), obtained using Gene Set Enrichment Analysis. ***P<0.001. ERH, enhancer of rudimentary homolog; LUAD, lung adenocarcinoma; EMT, epithelial-mesenchymal transition; NSCLC, non-small cell lung cancer; NES, normalized enrichment score.

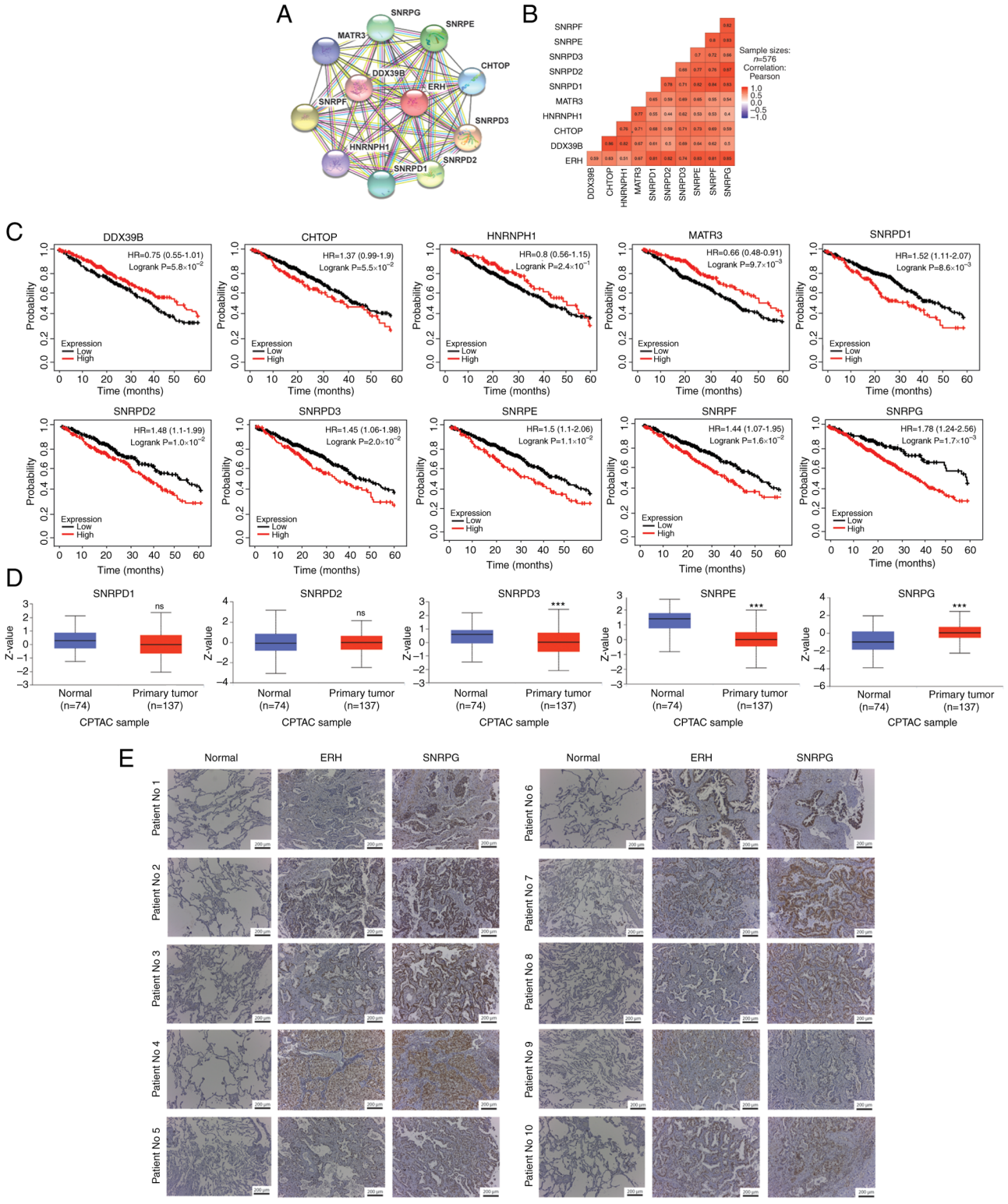

Figure 4. SNRPG and its potential interacting molecules with ERH. (A) Ten molecules potentially interacted with ERH using data from the STRING database. (B) The correlations between ERH and each candidate gene at the mRNA level in the LUAD cohort of TCGA. (C) Survival analysis of DOX39B, CHTOP, HNRNPH1, MATR3, SNRPD1, SNRPD2, SNRPD3, SNRPE, SNRPF and SNRPG. (D) Validation of the survival-associated molecules in tumor and non-tumor parts using data from the CPTAC database. (E) Immunohistochemistry staining of ERH and SNRPG collected from the in-house paired LUAD samples, magnification x10. ***P<0.001; NS, non-significant; SNRPG, small nuclear ribonucleoprotein polypeptide G; ERH, enhancer of rudimentary homolog; CPTAC, Clinical Proteomic Tumor Analysis Consortium; HR, hazard ratio.

ERH negatively correlated gene set correlated with the infiltration of cells such as CD4 T cells, follicular helper T cells, natural killer T (NKT) cells and natural killer (NK) cells (Fig. 6K). Based on the aforementioned findings, *ERH* and its correlated genes expressed in LUAD were associated with the infiltration of immune-suppressive cells, such as MDSCs and nTregs, which led to a microenvironment against immune surveillance.

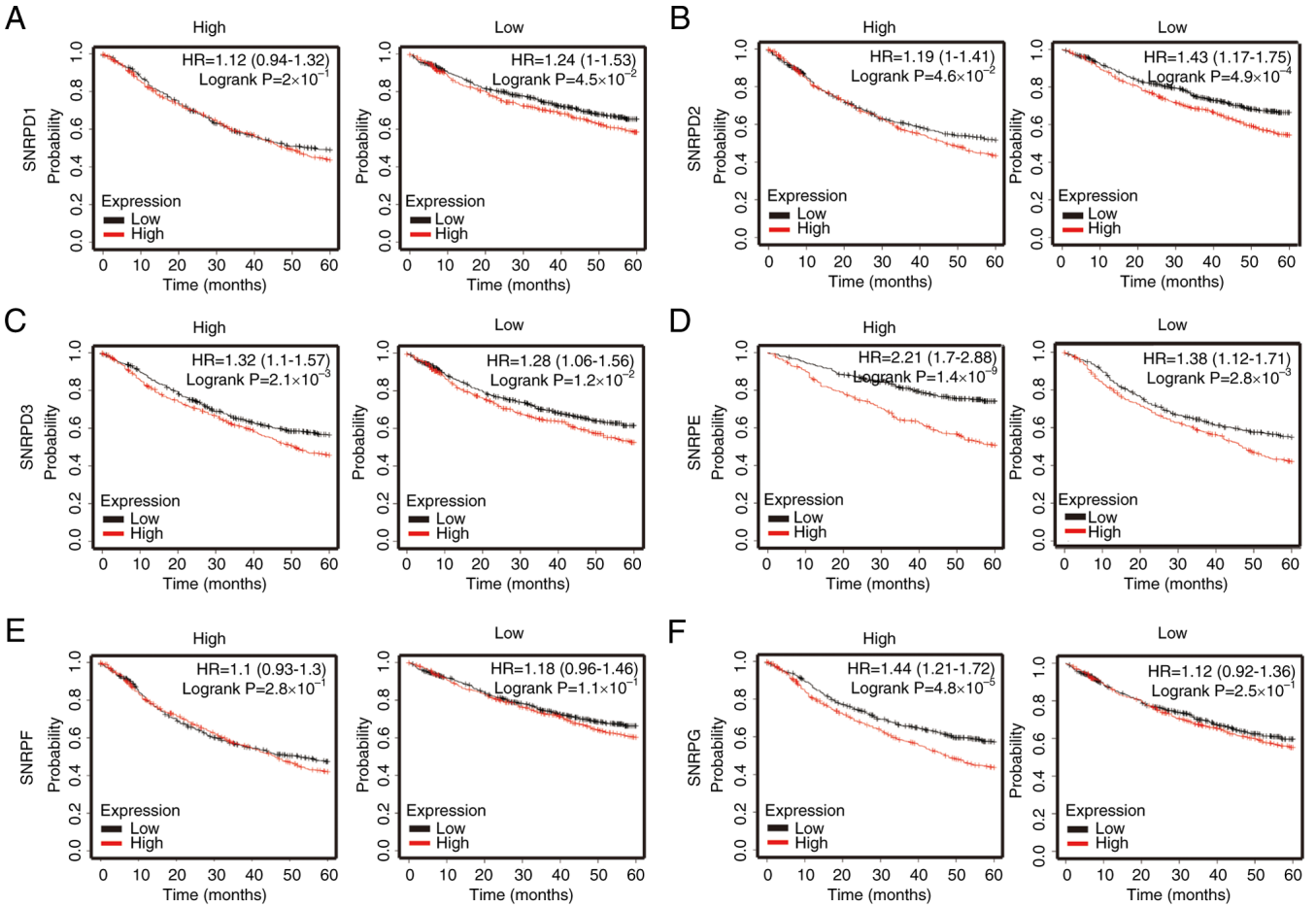

Figure 5. Effect of ERH on survival based on SNRPG expression using cross-analysis. (A) Cross-analysis between ERH and either high or low expression of SNRPD1, (B) SNRPD2, (C) SNRPD3, (D) SNRPE, (E) SNRPF and (F) SNRPG. ERH, enhancer of rudimentary homolog; SNRPG, small nuclear ribonucleoprotein polypeptide G.

ERH promotes EMT and cell migration in vitro. GSEA revealed an association between high *ERH* expression and cancer EMT and invasiveness. To validate the findings *in vitro*, cellular functional studies were designed using siRNAs to knock down *ERH* with high knockdown efficiency (Fig. 7A). There was no significant difference in the proliferation of A549 and CL1-0 cells with *ERH* knockdown compared with that of the control cells (Fig. 7B). To evaluate cell migration, Transwell migration and wound healing assays were performed, with the percentage of migrated cells and the distance of migration both significantly reduced in *ERH*-knockdown A549 and CL1-0 cells (Fig. 7C and D). These data supported the potential of *ERH* to enhance cell migration. Concerning EMT, the expression of mesenchymal markers, such as N-cadherin and vimentin, notably declined, whereas the epithelial marker E-cadherin was slightly elevated in *ERH*-knockdown A549 and CL1-0 cells (Fig. 7E). These results suggested that *ERH* regulated promotion and progression steps in LUAD, but not proliferation.

Discussion

To identify potential cures for lung cancer, more research efforts into the underlying mechanism of lung cancer and drug discovery are required. In the present study, *ERH* was demonstrated to be highly expressed in LUAD and was significantly associated with a poor prognosis. Meanwhile, upregulated *ERH* and its correlated gene set were linked to LUAD progression via control of the cell cycle, proliferation, invasion, EMT and metastasis. In addition, *ERH* was enriched in an immune suppressive microenvironment with a high fraction of MDSCs and nTregs. The *SNRPG* was the most critical interactive molecule which mediated the effects of *ERH* as the survival influence of *ERH* was likely reliant on an *SNRPG*-dependent mechanism. Therefore, *ERH* could be a potential target for LUAD treatment and manipulation of *ERH* and its interactive partner, *SNRPG*, could alter LUAD cellular behaviors and the immune microenvironment, consequently enhancing the sensitivity of immunotherapy.

Although *ERH*-related proliferation, invasion and migration have been previously studied in numerous cancer types (15,16), previous reports of the role of *ERH* in lung cancer are limited. To the best of our knowledge, only one previous study has reported the retarded growth of lung cancer cells resulting from the reduction of *ERH* and this was mediated by microRNA-574-3p over-expression secondary to irradiation *in vitro* (30). In the present study, it was proposed that functions of *ERH* might promote LUAD via cell cycle progression, proliferation, invasion, EMT and metastasis as determined by bioinformatics analysis. *ERH*-associated cellular behaviors

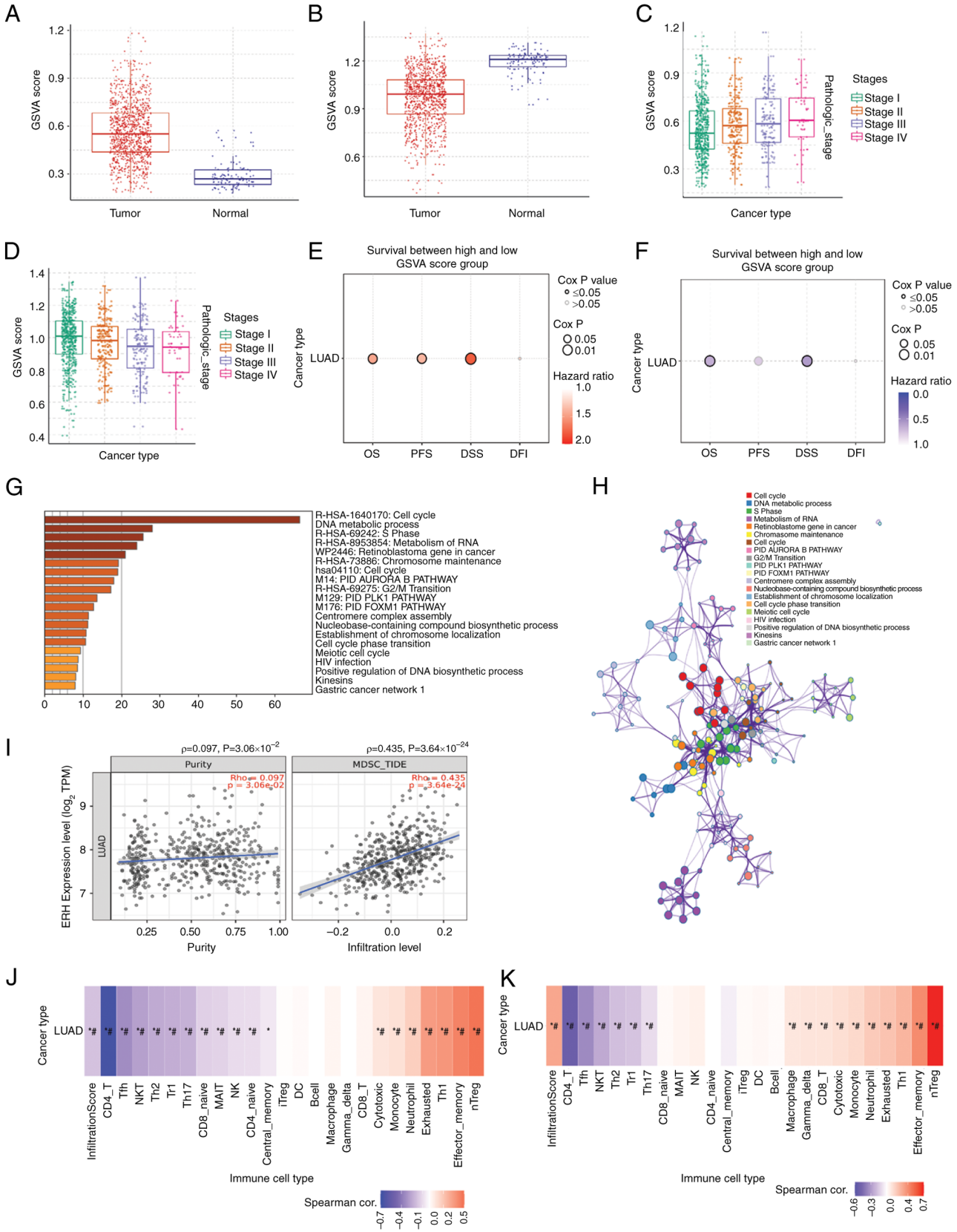

Figure 6. ERH positively correlated gene set is associated with worse survival and an immunosuppressive tumor microenvironment. (A) The GSVA score of the ERH positively correlated gene and (B) ERH negatively correlated gene set between LUAD tumor samples and normal samples. The association between the advanced stage and GSVA score of (C) the ERH positively correlated gene or (D) the ERH negatively correlated gene set. The association between survival analysis and GSVA score of (E) the ERH positively correlated gene set or (F) the ERH negatively correlated gene set. (G) The biological processes associated with the ERH positively correlated gene set, using data from the Metascape database. (H) The ERH-associated gene clusters using an enriched ontology cluster network. (I) Infiltration of myeloid-derived suppressor cells in tumors based on ERH expression using TIMER2.0. Infiltrating immune cells corresponding to the GSVA score of the ERH (J) positively- and (K) negatively-correlated gene sets. *P≦0.05; #FDR≦0.05. ERH, enhancer of rudimentary homolog; GSVA, Gene Set Variation Analysis; LUAD, lung adenocarcinoma; Tfh, T follicular helper; NKT, natural killer T; Th2, T helper 2; Tr1, Type 1 regulatory; Th17, T helper 17; MAIT, mucosal-associated invariant; NK, natural killer; iTreg, induced regulatory T; DC, dendritic; Th1, T helper 2; nTreg, natural regulatory T.

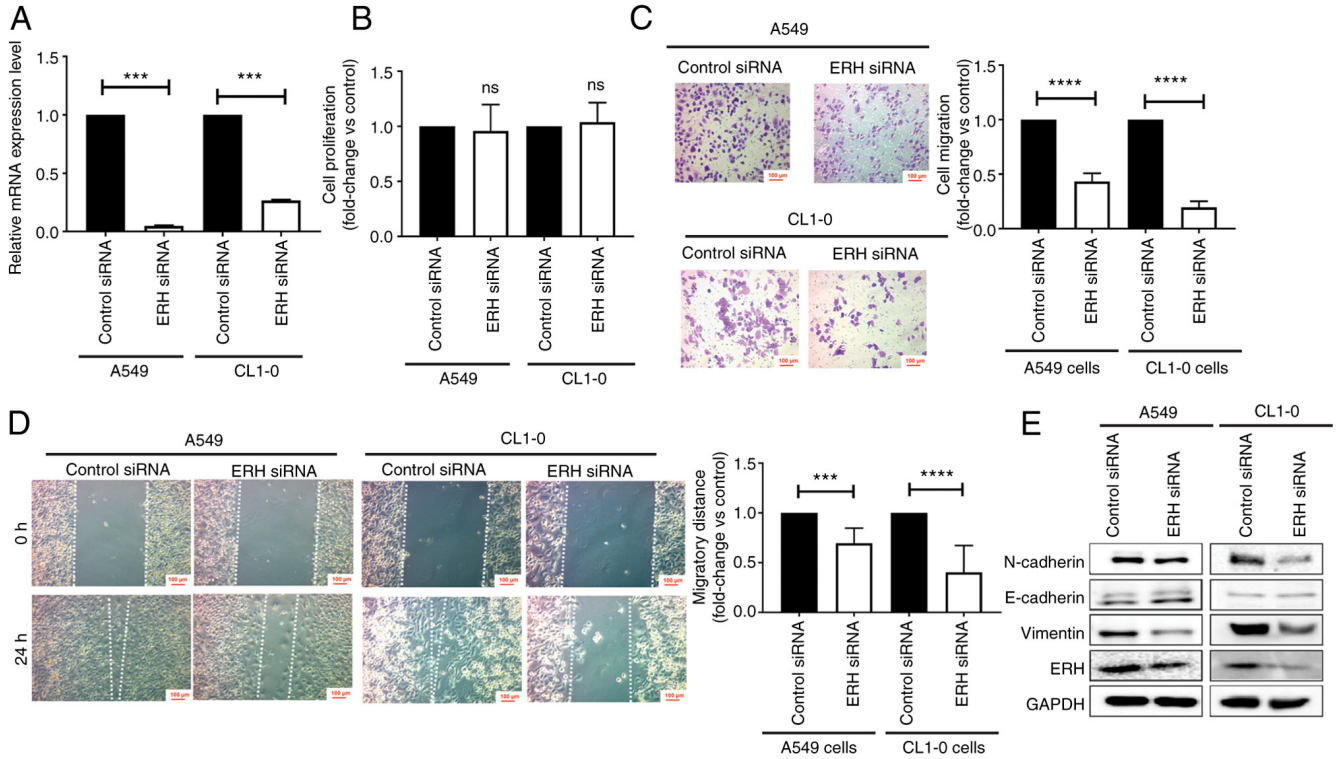

Figure 7. ERH facilitates cell migration and promotes epithelial-mesenchymal transition *in vitro*. The biological functions of ERH after knockdown of A549 and CL1-0 cells using siRNA method. (A) The knockdown efficiency of ERH siRNA in A549 and CL1-0 cells, respectively. (B) Proliferation assay, (C) Transwell migratory ability, (D) wound healing assays, and (E) epithelial-mesenchymal transition. Each experiment was repeated independently at least three times. ERH, enhancer of rudimentary homolog. ***P<0.005; ****P<0.001. ns, non-significance.

were assessed using A549 and CL1-0 cells, and the knockdown of *ERH* reduced cancer cell migratory ability and reversed the expression pattern of EMT markers. *ERH* has been linked to cellular proliferation (30,31), however the present study did not observe that knockdown of *ERH* affected cellular proliferation. Silencing of *ERH* led to reduced migration in the present study, which is compatible with the effects of *ERH* on tumor cell promotion and progression in bladder cancer (15) and ovarian cancers (16). These results add to the knowledge concerning lung cancer behaviors.

The TME is critical in the formation of immunity, tumor progression and metastasis, where chronic inflammatory status might alter immune cell adaptation which imbalances anti-cancer activity and favors immune evasion (32). MDSCs and Tregs serve major roles in tumor-associated immunosuppression and are associated with poor clinical outcomes in patients with lung cancer (33). In the present study, the observations of *ERH* overexpression and the immune-suppressive microenvironment were also unprecedented. First, *ERH* gene expression was demonstrated to be positively correlated with the infiltration of MDSCs in tumors using TIMER2.0. Second, the infiltrating immune cells corresponding to the GSVA score of the *ERH* positively correlated gene set were nTregs. Finally, the *ERH* negatively correlated gene set correlated with the infiltration of cancer killing NKT and NK cells. *ERH* was also demonstrated to have influenced the infiltration of immune cells in the lung cancer microenvironment, where high *ERH* expression was associated with a high percentage of MDSCs and nTregs. In contrast, low *ERH* expression was related to a high percentage of NKT and NK cells. Therefore, downregulation of *ERH* might increase infiltration and functions of NKT/NK cells in lung cancer, thereby improving the disease outcome of LUAD patients.

SNRPG, also termed as Smith Protein G, belongs to the *SNRP* family which constructs the main unit of spliceosomes and manages mRNA splicing (34). SNRPG is a part of the U1, U2, U4 and U5 small nuclear ribonucleoprotein (snRNP) complexes, whilst SNRPG is reportedly also a component of the U7 snRNP complex that takes part in the splicing of the 3' end of histone transcripts (35). Therefore, both *ERH* and SNRPs might be involved in the RNA splicing process. Previously, *ERH* was reported to interact with SNRPD3 for splicing of CENP-E in the context of KRAS-mutant cancer cells. Interference in CENP-E RNA splicing leads to the defects of chromosome congression, hampering further cell cycle progress and proliferation (14). In the present study, numerous SNRPs interacting with *ERH* were identified using the STRING website. Among these, only *SNRPG* was positively correlated with *ERH* expression, at both mRNA and protein expression levels, as demonstrated by data from the TCGA and CPTAC databases, respectively. Moreover, the survival impact of *ERH* was only seen in cells with high *SNRPG* expression, which indicated an *SNRPG*-dependent modulating process. The results of the present study suggest the *ERH*-SNRPG interaction could serve a role in lung cancer treatment. There are limitations of the present study and further validation is required. First, the protein-protein interaction between ERH and SNRPG should be confirmed by co-immunoprecipitation. Second, the influence of *ERH* on MDSC infiltration in the tumor immune ecosystem should be validated by IHC staining.

To conclude, the prognosis for lung cancer is poor and novel therapies are worthy of investigation. The results from the present study demonstrated that *ERH* may serve a critical role in promotion, progression and alteration of the tumor-immune microenvironment. Therefore, drugs targeting *ERH* would be worth investigating and developing.

Acknowledgements

Not applicable.

Funding

This study was supported by grants from the Ministry of Science and Technology (grant nos. MOST 110-2314-B-037-124-MY3, MOST 110-2314-B-037-126-MY2 and MOST 111-2314-B-037-089), the Kaohsiung Medical University Hospital Research Funding (grant nos. KMUH-108-8R15, KMUH-110-0R14, and KMUH-110-0R17) and the Kaohsiung Municipal Ta-Tung Hospital Research Funding (grant no. KMTTH-110TA-04).

Availability of data and materials

The data generated in the present study can be accessed from the National Center for Biotechnology Information Gene Expression Omnibus (accession number, GSE236816) (https://www.ncbi.nlm.nih.gov/geo/query/acc.cgi?acc=GSE236816). All other datasets used and/or analyzed during the current study are available from the corresponding author on reasonable request.

Authors' contributions

YMT and JYH conceptualized the present study. YYW, YCH, CYC, YYC and LXL provided technical support, performed the experiments and acquired the data. YMT, KLW and JYH confirmed the authenticity of all of the raw data. CYC and HHC provided the software management and analyzed the data. YMT and KLW performed the formal analysis. JYH pursued the investigation and provided the resources. YMT, KLW and JYH performed data curation and interpreted the data. YMT and KLW wrote the original draft. JYH wrote, reviewed and edited the final manuscript. JYH supervised the study, was the project administrator and acquired the funding. All authors have read and approved the final manuscript.

Ethics approval and consent to participate

The protocol of the present study was approved [approval nos. KMUH-IRB-20180023, KMU-IRB-20200038 and KMU-IRB-E (II)-20220175] by the Institutional Review Board of Kaohsiung Medical University Hospital (Kaohsiung, Taiwan) and written informed consent was acquired from all enrolled patients.

Patient consent for publication

Not applicable.

Competing interests

The authors declare that they have competing interests.

References

1. Sung H, Ferlay J, Siegel RL, Laversanne M, Soerjomataram I, Jemal A and Bray F: Global cancer statistics 2020: GLOBOCAN estimates of incidence and mortality worldwide for 36 cancers in 185 countries. CA Cancer J Clin 71: 209-249, 2021.
2. Skřičková J, Kadlec B, Venclíček O and Merta Z: Lung cancer. Cas Lek Cesk 157: 226-236, 2018.
3. Bonney A, Malouf R, Marchal C, Manners D, Fong KM, Marshall HM, Irving LB and Manser R: Impact of low-dose computed tomography (LDCT) screening on lung cancer-related mortality. Cochrane Database Syst Rev 8: CD013829, 2022.
4. Deb D, Moore AC and Roy UB: The 2021 global lung cancer therapy landscape. J Thorac Oncol 17: 931-936, 2022.
5. Singh N, Temin S, Baker S Jr, Blanchard E, Brahmer JR, Celano P, Duma N, Ellis PM, Elkins IB, Haddad RY, *et al*: Therapy for stage IV non-small-cell lung cancer without driver alterations: ASCO living guideline. J Clin Oncol 40: 3323-3343, 2022.
6. Nicholson AG, Tsao MS, Beasley MB, Borczuk AC, Brambilla E, Cooper WA, Dacic S, Jain D, Kerr KM, Lantuejoul S, *et al*: The 2021 WHO classification of lung tumors: Impact of advances since 2015. J Thorac Oncol 17: 362-387, 2022.
7. Luo YH, Liang KH, Huang HC, Shen CI, Chiang CL, Wang ML, Chiou SH and Chen YM: State-of-the-art molecular oncology of lung cancer in Taiwan. Int J Mol Sci 23: 7037, 2022.
8. Isomura M, Okui K, Fujiwara T, Shin S and Nakamura Y: Cloning and mapping of a novel human cDNA homologous to DROER, the enhancer of the *Drosophila melanogaster* rudimentary gene. Genomics 32: 125-127, 1996.
9. Weng MT and Luo J: The enigmatic ERH protein: Its role in cell cycle, RNA splicing and cancer. Protein Cell 4: 807-812, 2013.
10. Krzyzanowski MK, Kozlowska E and Kozlowski P: Identification and functional analysis of the erh1(+) gene encoding enhancer of rudimentary homolog from the fission yeast Schizosaccharomyces pombe. PLoS One 7: e49059, 2012.
11. Wang X, Xie H, Zhu Z, Zhang J and Xu C: Molecular basis for the recognition of CIZ1 by ERH. FEBS J 290: 712-723, 2023.
12. Fang W and Bartel DP: MicroRNA clustering assists processing of suboptimal MicroRNA hairpins through the action of the ERH protein. Mol Cell 78: 289-302.e6, 2020.
13. Zhang Y, Wang X, Wang H, Jiang Y, Xu Z and Luo L: Elevated small nuclear ribonucleoprotein polypeptide an expression correlated with poor prognosis and immune infiltrates in patients with hepatocellular carcinoma. Front Oncol 12: 893107, 2022.
14. Weng MT, Lee JH, Wei SC, Li Q, Shahamatdar S, Hsu D, Schetter AJ, Swatkoski S, Mannan P, Garfield S, *et al*: Evolutionarily conserved protein ERH controls CENP-E mRNA splicing and is required for the survival of KRAS mutant cancer cells. Proc Natl Acad Sci USA 109: E3659-E3667, 2012.
15. Pang K, Zhang Z, Hao L, Shi Z, Chen B, Zang G, Dong Y, Li R, Liu Y, Wang J, *et al*: The ERH gene regulates migration and invasion in 5637 and T24 bladder cancer cells. BMC Cancer 19: 225, 2019.
16. Zhang D, Chu YJ, Song KJ, Chen YL, Liu W, Lv T, Wang J, Zhao H, Ren YZ, Xu JX, *et al*: Knockdown of enhancer of rudimentary homolog inhibits proliferation and metastasis in ovarian cancer by regulating epithelial-mesenchymal transition. Biomed Pharmacother 125: 109974, 2020.
17. Park JH, Park M, Park SY, Lee YJ, Hong SC, Jung EJ, Ju YT, Jeong CY, Kim JY, Ko GH, *et al*: ERH overexpression is associated with decreased cell migration and invasion and a good prognosis in gastric cancer. Transl Cancer Res 9: 5281-5291, 2020.
18. Park C, Lee WS, Go SI, Jeong SH, Yoo J, Cha HJ, Lee YJ, Kim HS, Leem SH, Kim HJ, *et al*: Apoptotic effects of anthocyanins from vitis coignetiae pulliat are enhanced by augmented enhancer of the rudimentary homolog (ERH) in human gastric carcinoma MKN28 cells. Int J Mol Sci 22: 3030, 2021.
19. Pang K, Li ML, Hao L, Shi ZD, Feng H, Chen B, Ma YY, Xu H, Pan D, Chen ZS and Han CH: ERH gene and its role in cancer cells. Front Oncol 12: 900496, 2022.
20. Blandin Knight S, Crosbie PA, Balata H, Chudziak J, Hussell T and Dive C: Progress and prospects of early detection in lung cancer. Open Biol 7: 170070, 2017.

21. Livak KJ and Schmittgen TD: Analysis of relative gene expression data using real-time quantitative PCR and the 2(-Delta Delta C(T)) method. Methods 25: 402-408, 2001.
22. Lim WK, Wang K, Lefebvre C and Califano A: Comparative analysis of microarray normalization procedures: Effects on reverse engineering gene networks. Bioinformatics 23: i282-i288, 2007.
23. Ghufran SM, Sharma P, Roy B, Jaiswal S, Aftab M, Sengupta S, Ghose S and Biswas S: Transcriptome wide functional analysis of HBx expressing human hepatocytes stimulated with endothelial cell cross-talk. Genomics 115: 110642, 2023.
24. Liu CJ, Hu FF, Xia MX, Han L, Zhang Q and Guo AY: GSCALite: A web server for gene set cancer analysis. Bioinformatics 34: 3771-3772, 2018.
25. Zhou Y, Zhou B, Pache L, Chang M, Khodabakhshi AH, Tanaseichuk O, Benner C and Chanda SK: Metascape provides a biologist-oriented resource for the analysis of systems-level datasets. Nat Commun 10: 1523, 2019.
26. Li T, Fu J, Zeng Z, Cohen D, Li J, Chen Q, Li B and Liu XS: TIMER2.0 for analysis of tumor-infiltrating immune cells. Nucleic Acids Res 48 (W1): W509-W514, 2020.
27. Saadoun S, Papadopoulos MC, Watanabe H, Yan D, Manley GT and Verkman AS: Involvement of aquaporin-4 in astroglial cell migration and glial scar formation. J Cell Sci 118: 5691-5698, 2005.
28. Chang WA, Yen MC, Hung JY, Yang CJ, Jian SF, Yeh IJ, Liu KT, Hsu YL and Kuo PL: Investigation of the role of tumor necrosis factor-like weak inducer of apoptosis in non-small cell lung cancer. Oncol Rep 39: 573-581, 2018.
29. Liu CJ, Hu FF, Xie GY, Miao YR, Li XW, Zeng Y and Guo AY: GSCA: An integrated platform for gene set cancer analysis at genomic, pharmacogenomic and immunogenomic levels. Brief Bioinform 24: bbac558, 2023.
30. Ishikawa K, Ishikawa A, Shoji Y and Imai T: A genotoxic stress-responsive miRNA, miR-574-3p, delays cell growth by suppressing the enhancer of rudimentary homolog gene in vitro. Int J Mol Sci 15: 2971-2990, 2014.
31. Fujimura A, Kishimoto H, Yanagisawa J and Kimura K: Enhancer of rudimentary homolog (ERH) plays an essential role in the progression of mitosis by promoting mitotic chromosome alignment. Biochem Biophys Res Commun 423: 588-592, 2012.
32. Quail DF and Joyce JA: Microenvironmental regulation of tumor progression and metastasis. Nat Med 19: 1423-1437, 2013.
33. Binnewies M, Roberts EW, Kersten K, Chan V, Fearon DF, Merad M, Coussens LM, Gabrilovich DI, Ostrand-Rosenberg S, Hedrick CC, *et al*: Understanding the tumor immune microenvironment (TIME) for effective therapy. Nat Med 24: 541-550, 2018.
34. Mabonga L and Kappo AP: The oncogenic potential of small nuclear ribonucleoprotein polypeptide G: A comprehensive and perspective view. Am J Transl Res 11: 6702-6716, 2019.
35. Bucholc K, Aik WS, Yang XC, Wang K, Zhou ZH, Dadlez M, Marzluff WF, Tong L and Dominski Z: Composition and processing activity of a semi-recombinant holo U7 snRNP. Nucleic Acids Res 48: 1508-1530, 2020.